Acoustic wave measurements on SNGS crystals and determination of material constants

E. Chilla[1], R. Kunze[2], M. Weihnacht[2], J. Bohm[3], R.B. Heimann[3], M. Hengst[3], U. Straube[4]

[1]*VI Tele Filter, Teltow, Germany, Email: chilla@telefilter.com*

[2]*IFW Dresden, D-01069 Dresden, Germany, Email: whn@ifw-dresden.de*

[3]*University of Mining and Technology, Freiberg, Germany, Email: heimann@mineral.tu-freiberg.de*

[4]*Martin-Luther-University, Halle, Germany, Email: u.straube@physik.uni-halle.de*

Introduction

Single crystals of compounds of calcium gallium germanate (CGG) structure with the general formula $A_3BC_3D_2O_{14}$, have been discussed as promising new materials for acoustic device applications. Since the CGG (or langasite) family belongs to the same acentric crystal class 32 as quartz similar acoustic properties can be expected. In particular, temperature compensated crystal cuts were predicted where the phase velocity of the acoustic wave is almost independent of temperature variation. Due to the larger piezoelectric coefficients these materials have a higher electromechanical coupling coefficient than quartz. Additionally, in contrast to quartz, where the temperature range of application is limited due to a structural phase transition, langasite-type crystals show structural stability up to the melting point. This offers the opportunity of SAW application at elevated temperatures, especially in sensing devices. The langasite-type crystals, i.e. LGS, LGN, and LGT, have been investigated intensively for some years. These materials, however, show statistical occupation of the cation positions. Recently ordered CGG materials found quite some interest. $Sr_3NbGa_3Si_2O_{14}$ (SNGS) exhibits ordered symmetry with all structurally distinct sites occupied by dissimilar atoms.

Here we report on the determination of the material properties of SNGS. The elastic constants were determined from measurements of the sound velocity of bulk acoustic waves (BAWs) and surface acoustic waves (SAWs).

Bulk acoustic waves

A widely used method for the recovery of the elastic constants is based on the phase velocity measurement of bulk acoustic waves along certain directions where an analytical solution of the wave equation can be found. Then, the influence of the various elastic parameters on the velocity can be separated from each other.

Hence, in a first step, we have extracted the elastic constants from bulk velocity data. We used *X*- and *Y*-cut quartz transducers of 20 MHz center frequency to generate longitudinal and transverse sound waves in the SNGS crystal. These quartz transducers were bonded with epoxy resin to the sample.

The measurement of the sound velocity was carried out using the conventional pulse-echo method [1]. The reflected rf echo signals are superimposed on an oscilloscope using a fast trigger frequency that corresponds to the signal delay from the transducer to the sample end face and back. The delay time can be found from the trigger frequency and has an accuracy of about 10^{-4}. In addition a systematic error appears from the thickness variation of the epoxy resin. Hence, an uncertainty of about 1 % for the reported velocity measurements is estimated. The acoustic measurements were carried out on samples oriented with their edges (i) parallel to the *X*, *Y*, *Z*-axes, and (ii) rotated by 45° around the X-axis (crystallographic [011]-direction). From the velocities of sound propagation the elastic stiffness coefficients c_{ij} were derived using the system of equations published in [2, 3].

Dielectric measurements were performed using a General Radio 1621 Precision Capacitance Measurement System at a frequency of 800 Hz. An equipment based on a capacitive detector was used for measurements of the piezoelectric strain coefficients d_{ij} [4].

From the velocity data of the bulk acoustic waves, the piezoelectric and dielectric constants we derived a set of elastic stiffness coefficients for SNGS. When using these parameters for the calculation of the angular SAW dispersion, however, a deviation with respect to the measured data of up to 5 % was found, which is much higher than the experimental uncertainty. Hence, additional optimization has to be performed regarding the measured angular SAW dispersion.

Surface acoustic waves

The SAW measurements were performed using thermoelastic SAW excitation and mechanical detection [5]. The SAWs were excited by a 0.5 ns laser pulse with 0.5 mJ pulse energy generated by a Nitrogen laser with a wavelength of 337 nm line-focused at the sample surface. The sketch of the experimental setup is shown in Figure 1.

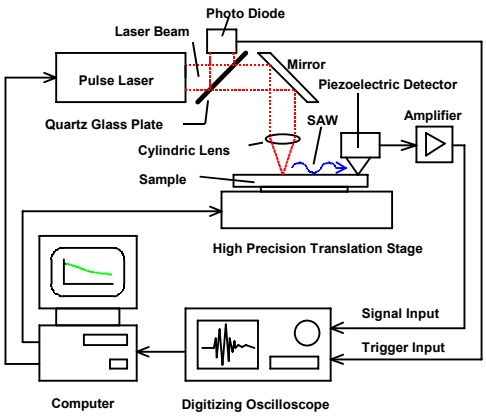

Figure 1: Setup for thermoelastic measurement

For non-transparent materials the energy is absorbed as heat into a small volume at the sample surface. The rapid expansion and contraction of the heated volume generates an acoustic wave pulse propagating through the sample. Most

of the energy goes into surface guided acoustic waves. The normal component of the mechanical vibrations are converted to a voltage after certain propagation distances in a piezoelectric polymer foil, amplified and stored by a digitizing oscilloscope. The sample is moved relative to the laser beam for defining the propagation ways. The SAW wave packets are detected over a typical frequency range of 20-250 MHz frequency due to the limited transduction bandwidth of the PVDF foil. The phase velocity is calculated from the phase spectra of the detected signals. The average measurement error was up to ±1 m/s. The samples were mounted on a computer controlled rotation stage to allow for measurement of angular dispersion of SAW phase velocity.
Since SNGS is almost transparent at 337 nm, the samples were coated with a 50 nm thick Al layer (*X*-cut) and 10 nm thick Ti layer (*Y*-cut), respectively, to increase the absorption efficiency. Consequently, for accurate velocity calculations the slowing-down effect of SAW by short-circuiting must be considered. Furthermore a 10 nm thick tetragonal amorphous carbon (ta-C) layer was evaporated by the filtered vacuum arc deposition method [6] to allow also for SAW excitation on open-circuited surface. This gives the opportunity to

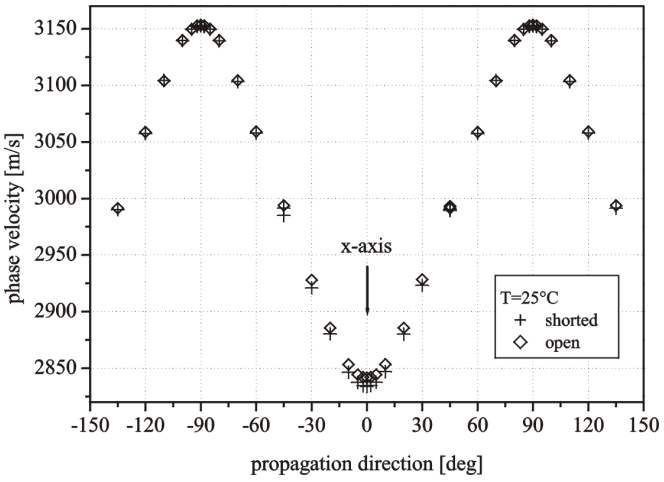

Figure 2: Angular dispersion at *Y*-cut SNGS. Crosses denote measurement for metallized surface (10 nm Ti) and diamonds denote open-circuited surface (10 nm ta-C layer).

directly determine the electromechanical coupling coefficient which is given as twice the relative velocity difference of open- and short-circuited surfaces. The angular phase velocity dispersion has been measured for *X*-, *Y*-, and *Z*-cut of SNGS. In Figure 2 the measured data for the short-circuited *Y*-cut surface (10 nm Ti layer) and the open-circuited (10 nm ta-C layer) are shown.

Material constants recovery

The evaluation of the material parameters was carried out based on the data set obtained from BAW measurements. For the material determination constants we used a multidimensional optimisation procedure. For the solution of the inverse problem we analyzed the SAW data from the *X*-, *Y*-, and *Z*-cut measurements. Additionally we used c_{11}, c_{33}, and c_{44} recovered from bulk wave measurements. In Table 2 the final material constants of SNGS are displayed.

density $\rho\,[kg/m^3]$	4650
dielectric constants	
$\varepsilon_1/\varepsilon_0$	12.4
$\varepsilon_3/\varepsilon_0$	21.4
piezoelectric constants $[C/m^2]$	
e_{11}	0.486
e_{14}	0.10
piezoelectric constants $[GPa]$	
c_{11}	160.8
c_{12}	74.0
c_{13}	82.3
c_{14}	4.5
c_{33}	202.2
c_{44}	55.3

Table 2: Material constants of SNGS.

Using this set of material constants the SAW parameters relevant for device application like coupling coefficient, power flow angle, diffraction coefficient, reflection coefficient have been calculated. Usually, they are given as functions of substrate orientation within the crystallographic coordinate system described by Euler angles (subsequent rotation around *Z*-, *X*-, *Z*-axes of substrate). As an example the contour plot of SAW coupling coefficient as a function of 2nd and 3rd Euler angle is shown in Figure 3. Comparatively, for this sector the coupling coefficient of quartz is roughly four times smaller.

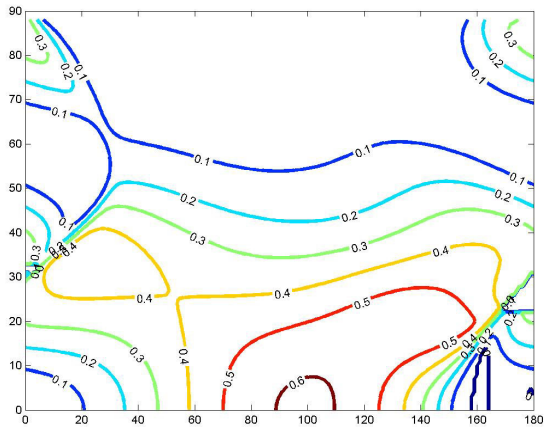

Figure 3: Contour map of SAW coupling coefficient (in %) vs. 2nd (abscissa) and 3rd (ordinate) Euler angle.

References

[1] E.P. Papadakis, J. Acoust. Soc. Am. **42**, 1045 (1967).
[2] R. Truell, C. Elbaum, and B. Chick, *Ultrasonic Methods in Solid State Physics*, Academic Press, New York, 1969.
[3] E. Chilla, C. Flannery, H.-J. Fröhlich, U. Straube, J. Appl. Phys. **90**, 6084 (2001).
[4] G. Sorge, T. Hauke, M. Klee, Ferroelectrics **163**, 77 (1995).
[5] M. Weihnacht, K. Franke, K. Kämmer, R. Kunze, and H. Schmidt, Proc. 1997 IEEE Ultrason. Symp., 217 (1997).
[6] T. Witke, T. Schuelke, B. Schultrich, P. Siemroth, J. Vetter, Surface and Coatings Technology **126**, 81 (2000).